Advances in Nano Research, *Vol. 15, No. 3 (2023) 263-275*
https://doi.org/10.12989/anr.2023.15.3.263

Electron transport properties of Y-type zigzag branched carbon nanotubes

MaoSheng Ye[1], HangKong OuYang*[1], YiNi Lin[1], Quan Ynag[1],
QingYang Xu[1], Tao Chen[2], LiNing Sun[2] and Li Ma**[1]

[1]*School of Mechatronic Engineering and Automation, Shanghai University, Shanghai 200072, China*
[2]*Robotics and Microsystems Center, Soochow University, Suzhou 215021, China*

(*Received May 9, 2022, Revised April 5, 2023, Accepted April 7, 2023*)

Abstract. The electron transport properties of Y-type zigzag branched carbon nanotubes (CNTs) are of great significance for micro and nano carbon-based electronic devices and their interconnection. Based on the semi-empirical method combining tight-binding density functional theory and non-equilibrium Green's function, the electron transport properties between the branches of Y-type zigzag branched CNT are studied. The results show that the drain-source current of semiconducting Y-type zigzag branched CNT (8, 0)-(4, 0)-(4, 0) is cut-off and not affected by the gate voltage in a bias voltage range [-0.5 V, 0.5 V]. The current presents a nonlinear change in a bias voltage range [-1.5 V, -0.5 V] and [0.5 V, 1.5 V]. The tangent slope of the current-voltage curve can be changed by the gate voltage to realize the regulation of the current. The regulation effect under negative bias voltage is more significant. For the larger diameter semiconducting Y-type zigzag branched CNT (10, 0)-(5, 0)-(5, 0), only the value of drain-source current increases due to the larger diameter. For metallic Y-type zigzag branched CNT (12, 0)-(6, 0)-(6, 0), the drain-source current presents a linear change in a bias voltage range [-1.5 V, 1.5 V] and is symmetrical about (0, 0). The slope of current-voltage line can be changed by the gate voltage to realize the regulation of the current. For three kinds of Y-type zigzag branched CNT with different diameters and different conductivity, the current-voltage curve trend changes from decline to rise when the branch of drain-source is exchanged. The current regulation effect of semiconducting Y-type zigzag branched CNT under negative bias voltage is also more significant.
Keywords: electron transport properties; semi-empirical method; Y-type zigzag branched carbon nanotube

1. Introduction

Carbon nanotubes (CNTs) have excellent electrical and physical properties (Bai *et al*. 2018, Ding *et al*. 2018, Wang *et al*. 2020, Yang *et al*. 2021a, b, Lin *et al*. 2022). They are important research materials for nano electronic devices that are constantly miniaturized and integrated (Peng *et al*. 2019, Cheng *et al*. 2023, Guo *et al*. 2023, Huang *et al*. 2023b, Tang *et al*. 2023, Wu *et al*. 2023, Zhao *et al*. 2023). They have broad application prospects in the fields of microelectronics industry and integrated circuit semiconducting industry (Hills *et al*. 2019, Sun *et al*. 2019, Xu *et al*. 2020). Since the 20th century, traditional silicon-based electronic devices, as an important driving force for the scale-up of integrated circuits, have excellent performance in switching speed, operating energy consumption and manufacturing costs (Liu *et al*. 2021, Wang *et al*. 2021, Shen *et al*. 2022, Chen *et al*. 2023, Huang *et al*. 2023a). However, the short channel effect caused by the shrinking size of transistors makes it difficult for silicon-based field-effect transistors to meet the prediction of Moore's law. As a nearly perfect molecular level material, single-walled carbon nanotubes can be divided into metallic and semiconducting according to different conductive properties (Adamian *et al*. 2020, Al-Furjan *et al*. 2020a, b, Li *et al*. 2020, Zare *et al*. 2020, Dai *et al*. 2021). Among them, semiconducting single-walled carbon nanotubes are considered to be one of the best choices for field effect transistors channel materials because of their high electron mobility and ballistic transport (Javey *et al*. 2003, Durkop *et al*. 2004). Carbon nanotubes as channel materials need to be connected to external circuits through the metal electrodes formed by the photolithography process (Ebrahimi *et al*. 2017, Ghadiri *et al*. 2017c, Shahabinejad *et al*. 2018, Shafiei *et al*. 2020). The radial compression deformation (Martel *et al*. 1998, Ohnishi *et al*. 2016), the contact resistance (Pitner *et al*. 2019) and the contact strength with the gate (Wang *et al*. 2014) will affect the excellent electrical properties of carbon nanotubes, and it is difficult for the integrated circuits to meet the size requirements of nanocircuits (Xin *et al*. 2021, Zhao *et al*. 2021, Li *et al*. 2022, Zhao *et al*. 2022, Yang *et al*. 2023). Carbon nanotubes with different diameters and conductivity can be connected to form intramolecular metallic/semiconducting diodes through topological defects of pentagon and heptagon (Charlier *et al*. 1996, Chico *et al*. 1996), and the structure of heterojunction can be identified by differential current method (Ouyang *et al*. 2001). For typical two-terminal electronic devices, the conductivity can only be changed by applying electric field (Wang Yi-Jun and Cheng 2015) and magnetic field, while three-terminal electronic devices such as Y-type branched carbon nanotubes can use their own third branch to accurately control the current flowing

*Corresponding author, Ph.D.,
E-mail: hankow@shu.edu.cn
**Co-corresponding author, Ph.D.,
E-mail: malian@shu.edu.cn

ISSN: 2287-237X (Print), 2287-2388 (Online)

through the remaining two branches, and researchers have used catalytic pyrolysis (Chen *et al*. 2019), chemical vapor deposition (ChandraKishore and Pandurangan 2013) and the arc discharge method (Joseph Berkmans *et al*. 2014) to achieve high-yield preparation.

In recent years, three-terminal electronic devices have received extensive attention (Azimi *et al*. 2016, Ghadiri *et al*. 2016a, b, Shafiei *et al*. 2016, 2017). Due to the particularity of the structure of carbon materials, a number of researches have been carried out both at the three-terminal graphene and three-terminal carbon nanotubes. Araujo *et al*. (2021) have studied the ballistic transport properties of graphene Y-junctions, and realized the current regulation between the other two branches by controlling the refractive index of p-n junction through the third end gate potential. Using the finite element analysis method, Butti *et al*. (2013) simulated the rectification effect of the three-terminal graphene nanoribbon based on the carrier diffusion transport model in the field effect transistor, and studied the effects of the shape, temperature and potential disorder of the nanoribbon on the rectification efficiency. Using the non-equilibrium Green's function method, Gu Yun-Feng *et al*. (2016) verified the feasibility of the ballistic thermal rectification in the three-terminal graphene nano-junction, and proposed the method of using an inclined branch as the control terminal to cooperate with the left and right terminal to produce the ballistic thermal rectification, and studied the difference in thermal rectification between armchair and zigzag graphene nanojunction. Händel *et al*. (2014) studied the electron transport properties of T-type three-terminal graphene nanojunction, analyzed the relative position of horizontal and vertical branches and the influence of branch bandwidth on electron transport properties. Andriotis *et al*. (2001) calculated the quantum conductivity of Y-type branched carbon nanotubes, studied the effect of the angle between branches on the conductivity, and proposed the idea of using it as a molecular electronic switch. Park *et al*. (2006) used Y-type branched carbon nanotubes to study the effect of branch diameter on transconductance and output conductance. The research group believes that different branches of Y-type branched carbon nanotubes can be selected to form different conduction paths and applied to field programmable gate arrays (FPGAs) (Ehyaei *et al*. 2017, Ghadiri *et al*. 2017a, b, Shivanian *et al*. 2017). Bandaru *et al*. (2005) used the focused ion beam to deposit gold contacts on the three ends of Y-branch carbon nanotubes and connect platinum wires to test electrical performance. When two branches are connected to positive bias voltage at the same time, the third branch will output positive voltage, which can realize the function of an AND logic gates. However, the above studies on Y-type branched carbon nanotubes have not analyzed the effects of different diameters and different conductivity on the electron transport properties due to the limitation of experimental environment or computing resources (Hou *et al*. 2021, Huang *et al*. 2021, Xu *et al*. 2021, Wang *et al*. 2022).

In this paper, we construct Y-type zigzag branched carbon nanotubes by connecting single-walled carbon nanotubes with different diameters and different conductivity, the semi-empirical calculation method combining tight-binding density functional theory (DFTB) and non-equilibrium Green's function (NEGF) is used to systematically study the electron transport properties between the branches of Y-type zigzag branched carbon nanotubes, and analyze the feasibility of using it as a three-terminal nano electronic device, which is of great significance for the design and manufacture of carbon nanotube field effect transistors.

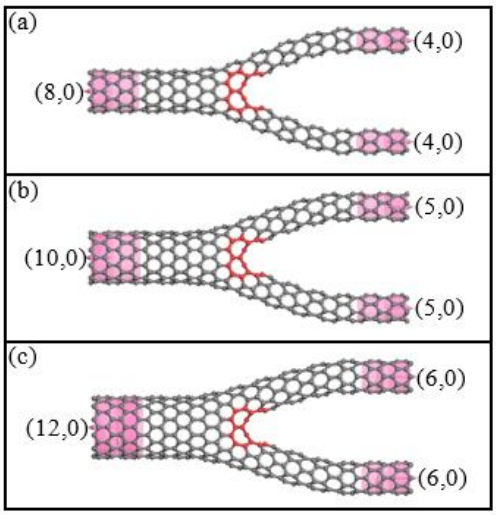

Fig. 1 The calculation model for the electron transport properties of Y-type branched carbon nanotube. Semi-conducting: (a) (8, 0)-(4, 0)-(4, 0), (b) (10, 0)-(5, 0)-(5, 0), Metallic: (c) (12, 0)-(6, 0)-(6, 0)

2. Model and calculation method

In this paper, Y-type zigzag branched carbon nanotubes with different diameters and different conductivity are built to study their electronic transport properties. Y-type zigzag branched carbon nanotubes are built by connecting two branches with smaller diameters and a trunk with a larger diameter, and the two branches form an acute angle. At the front side, back side and the middle of the connection, two heptagons (shown as red atoms in Fig. 1) are distributed separately to complement the negative curvature generated when carbon nanotubes of different diameters are connected, which can maintain the low-energy configuration of carbon atoms (Xue *et al*. 2008), and other structures are hexagons arranged in axial order. In this paper, semiconducting Y-type zigzag branched carbon nanotubes with different diameters (8, 0)-(4, 0)-(4, 0), (10, 0)-(5, 0)-(5, 0) and metallic Y-type zigzag branched carbon nanotubes (12, 0)-(6, 0)-(6, 0) are built. The length of the trunk and branch carbon nanotubes is six periods, two periods are selected at each end as the semi-infinite electrode, and the length of the middle scattering region is eight periods, as shown in Fig. 1.

The semi-empirical method (Seifert 2007, Kim and Kim 2008, Pecchia *et al*. 2008) combining DFTB and NEGF was used to optimize the structure and calculate the electron transport properties of Y-type zigzag branched carbon nanotubes, which were characterized by current-voltage curve and electron transmission spectrum. The structure of Y-type

Table 1 Scheme and parameter setting up in calculations

electronic state description and solution method	calculation method	parameter settings
geometry Optimization	algorithm	smart method
	convergence thresholds	energy 0.02 kcal / mol force 0.1 kcal / mol / Å stress 0.05 Gpa displacement 0.001 Å max. iterations 500
slater-Koster library	CHNO	
method for diagonalizing the Hamiltonian	divide and conquer	
delf-consistent calculations	delf consistent charge（SCC）	SCC tolerance 1×10-8 eV max. SCC cycles 500
	Broyden	mixing amplitude 0.05
k-pointsampling in Brillouin area	uniform distribution	0.02 / Å
Poisson solver	buffer length	7.5 Å
	max. grid spacing	0.5 Å
	boundary conditions with electrodes	Dirichlet
	boundary conditions with no electrodes	Neumann
	Electrode buffer length	0.3 Å
orbital occupation	smearing	0.001Ha

zigzag branched carbon nanotubes is relatively complex, and the calculation is time-consuming. Therefore, in this paper, the thermal smearing will be applied to the orbital occupation to speed up convergence. Fermi or Methfessel - Paxton are selected as the distribution functions when calculating semiconducting or metallic Y-type zigzag branched carbon nanotubes (Hamidi *et al*. 2015, Allahkarami *et al*. 2017, Ehyaei, Akbarshahi and Shafiei 2017, Akbas 2018, Akbaş 2018, Arefi and Zenkour 2018, Aydogdu *et al*. 2018, Bensaid *et al*. 2018, Navi *et al*. 2019, Ebrahimi *et al*. 2020, Gafour *et al*. 2020, Matouk *et al*. 2020). The specific calculation method and parameter settings are listed in Table 1.

In this paper, according to the mechanism of the field effect transistor, different voltages are applied to each branch of the Y-type zigzag branched carbon nanotube, so that the effect of different electrodes in the field effect transistor can be realized. The applied voltage settings are source voltage V_S = 0 V, drain voltage V_D = [-1.5 V, 1.5 V] and gate voltage V_G = -1V,0 V and 1 V. Calculate the current through each branch using the Landauer-Buttiker formula (Buttiker *et al*. 1985):

$$I_{ij} = \frac{2e}{h}\int_{-\infty}^{+\infty} dET_{ij}(E,V_b)[f(\mu_i) - f(\mu_j)] \quad (1)$$

where i, j is the branch number of carbon nanotubes, e represents the electron charge, h is the Planck constant, f represents the Fermi distribution function, μ is the electro-chemical potential of the electrode, and $T(E,V_b)$ represents the transmission coefficient when the bias voltage is V_b between the electrodes and the electron energy is E. If at low temperature,$f$can be approximated as a step function, which is zero at the Fermi level, so the effective interval of current integration in formula (1) is reduced from $[+\infty,-\infty]$ to $[\mu_i,\mu_j]$. $T(E,V_b)$ can be obtained by the following formula:

$$T_{ij}(E,V_b) = Tr[\Gamma_i G^R(E)\Gamma_j G^A(E)] \quad (2)$$

where Γ is the linewidth function of the electrode, $G^R(E)$ and $G^A(E)$ are the delayed and advanced Green's functions, respectively.

3. Results and discussion

In order to facilitate the analysis and understanding of the electronic transport properties of Y-type zigzag branched carbon nanotubes, the electronic density of states (DOS) of semiconducting single-walled carbon nanotubes (4, 0) and (8, 0), (5, 0) and (10, 0) and metallic single-walled carbon nanotubes (6, 0) and (12, 0) are given in Fig. 2(a)-(c), where the Fermi level is located at 0ev. As shown in Figs. 2(a) and 2(b), single wall carbon nanotubes (4, 0), (8, 0), (5, 0) and (10, 0) have energy gaps at the Fermi level, showing semiconducting, as shown in Fig. 2(c), single-walled carbon nanotubes (6, 0) and (12, 0) have no energy gap at the Fermi level and show metallic.

Firstly, the electronic transport properties between different branches of semiconducting Y-type zigzag branched carbon nanotubes are studied. The semiconducting Y-type zigzag branched carbon nanotubes (8, 0)-(4, 0)-(4, 0) built from single-walled carbon nanotubes (8, 0) and (4, 0)

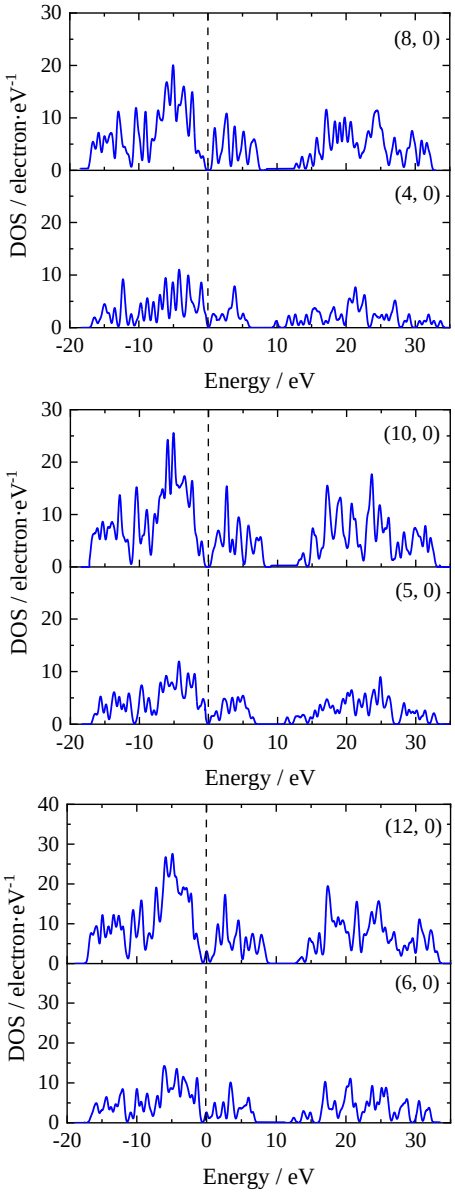

Fig. 2 The density of states of single-walled carbon nanotube. Semiconducting: (a) (4, 0) and (8, 0), (b) (5, 0) and (10, 0), Metallic: (c) (6, 0) and (12, 0)

with diameters of 6.26 and 3.13 respectively are selected as the research object. The current-voltage curves of source-drain on different branches are showed in Fig. 3, and the horizontal axis is the drain voltage V_D, the vertical axis is the current I_{DS} flowing through the drain-source, in which the blue triangle curve, red circle curve, and black square curve represent the applied gate voltages V_G of -1 V, 0 V, and 1 V respectively. The illustration in Fig. 3 reflects the relationship between the tangent slope k of the current-voltage curve and the drain voltage V_D when V_G is 0 V. In order to clearly express the current change trend, k is defined as the tangent slope of the current-voltage curve, which can be calculated by the following formula:

$$k = \lim_{\Delta V_D \to 0} \frac{\Delta I_{DS}}{\Delta V_D} \quad (3)$$

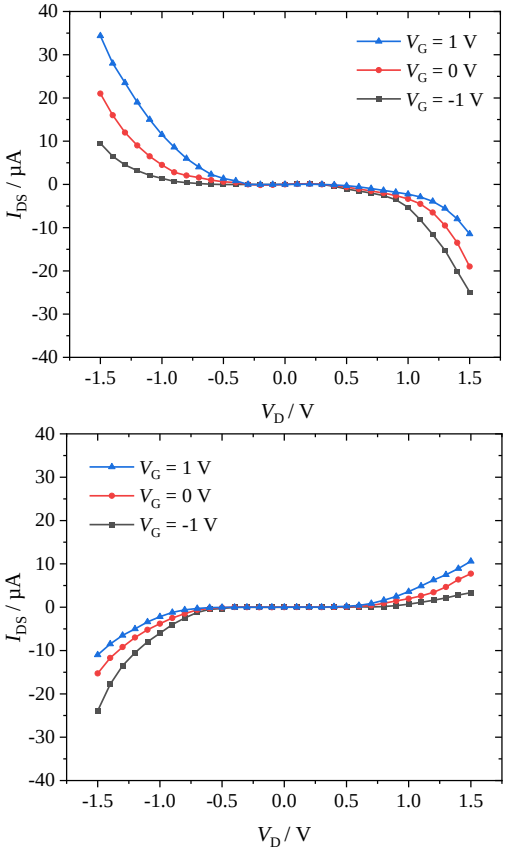

Fig. 3 The current-voltage(I-V) curve of semiconducting Y-type zigzag branched carbon nanotube (8, 0)-(4, 0)-(4, 0). (a) source, drain and gate: (8, 0), (4, 0) and (4, 0), and the inset shows the variation curve of k with V_D when V_G = 0 V, (b) source, drain and gate: (4, 0), (8, 0) and (4, 0), and the inset shows the variation curve of k with V_D when V_G = 0 V

where ΔV_D is the voltage increment taken on both sides of the current-voltage curve at a certain point, and ΔI_{DS} is the current increment when ΔV_D is taken.

The current-voltage curves in which the trunk (8, 0) is used as the source and the two branches (4, 0) are used as the drain and gate respectively are showed in Fig. 3(a), which shows a nonlinear downward trend as a whole. As the absolute value of drain voltage $|V_D|$ increases, the absolute value of tangent slope $|k|$ of the current-voltage curve continues to increase, as shown in the illustration in Fig. 3(a). In particular, within the range of V_D = [-0.5 V, 0.5 V], the current is in the cut-off state, that is, I_{DS} = 0 μA, and is not affected by V_G. When V_G takes different values, the changing trend of the current-voltage curves is significantly different. As shown by the red circular curve in Fig. 3 (a), when V_G = 0 V, the value of $|I_{DS}|$ under the maximum positive and negative bias voltages are both around 20 μA, and in the range of V_D = [-1.5 V, 1.5 V], both $|I_{DS}|$ and $|k|$ are symmetric about V_D = 0 V. As shown by the blue triangle curve in Fig. 3(a), when V_G = 1 V, in the range of V_D = [-1.5 V, -0.5 V], $|k|$ becomes larger, making the increment of $|I_{DS}|$ larger, in the range of V_D = [0.5 V, 1.5 V], |k| becomes smaller, making the increment of $|I_{DS}|$ smaller. Therefore, $|I_{DS}|$ and $|k|$ are no longer symmetric about V_D = 0 V, and

$|I_{DS}|$ under negative bias is larger than $|I_{DS}|$ under positive bias. As shown by the black square curve in Fig. 3(a), when V_G = -1 V, in the range of V_D = [-1.5 V, -0.5 V], $|k|$ becomes smaller, making the increment of $|I_{DS}|$ smaller, in the range of V_D = [0.5 V, 1.5 V], $|k|$ becomes larger, making the increment of $|I_{DS}|$ larger. Therefore, $|I_{DS}|$ and $|k|$ are no longer symmetrical about V_D = 0 V, and $|I_{DS}|$ under negative bias is smaller than $|I_{DS}|$ under positive bias. The results show that in the range of V_D = [-0.5 V, 0.5 V], the current is in the cut-off state and not controlled by the gate voltage, in the range of V_D = [-1.5 V, -0.5 V] and [0.5 V, 1.5 V], the gate voltage can regulate the current through the drain-source, especially in the negative bias range, the absolute value of the current flowing through the drain-source changes greatly in increments, and the regulation effect is more significant.

Swap the carbon nanotubes where the source and drain are located. The current-voltage curves in which the trunk (8, 0) is used as the drain and the two branches (4, 0) are used as the source and gate respectively are showed in Fig. 3(b), which shows a nonlinear upward trend as a whole. With the increase of $|V_D|$, the k of the current-voltage curve also increases continuously, as shown in the inset of Fig. 3(b). The branch positions where the drain and source are located are interchanged, and the current direction determination reference remains unchanged, so the overall change trend of the current changes from falling to rising. The same as Fig. 3(a) is: in the range of V_D = [-0.5 V, 0.5 V], the current is also in the cut-off state, that is, I_{DS} = 0 μA, which is not affected by V_G, In the range of V_D = [-1.5 V, -0.5 V], compared with V_G = 0 V, when V_G = -1 V (1 V), k will become larger (smaller), so that the increment of $|I_{DS}|$ will also become larger (smaller), in the range of V_D = [0.5 V, 1.5 V], compared with V_G = 0 V, when V_G = -1 V (1 V), k will become smaller (larger), so that the increment of $|I_{DS}|$ will also become smaller (larger), in particular, different from Fig. 3(a), when V_G = 0 V, $|I_{DS}|$ under the maximum positive and negative bias are 7.75 μA and -15.27 μ A respectively, which is no longer symmetrical about V_D = 0 V, but due to the change of k, when V_G = 1 V, $|I_{DS}|$ is exactly symmetrical about V_D = 0 V, and $|I_{DS}|$ under the maximum positive and negative bias are around 10 μA. These research results show that when the same regular voltage is applied to different branches of the same Y-type zigzag branched carbon nanotube, the electron transport properties are similar, and the gate voltage can also be used to control the current flowing through the drain-source, and the regulation effect is better in the range of negative bias voltage.

In order to further analyze the changing laws of the current-voltage curves in Figs. 3(a) and 3(b), the transmission spectrum of the trunk (8, 0) as the source and the two branches (4, 0) as the drain and gate when V_G takes 0 V, -1 V and 1 V respectively is showed in Fig. 4(a)-(c),the transmission spectrum of the trunk (8, 0) as the drain and the two branches (4, 0) as the source and gate when V_G takes 0 V, -1 V and 1 V respectively is showed Fig. 5(a)-(c). The Fermi level takes E = 0 eV as the energy reference point, and the bias window is [-V_D/2, V_D/2], that is, the area between the black dotted lines in Fig. 4 and Fig. 5. The current flowing through the drain-source can be obtained by integrating the transmission coefficient in the bias window.

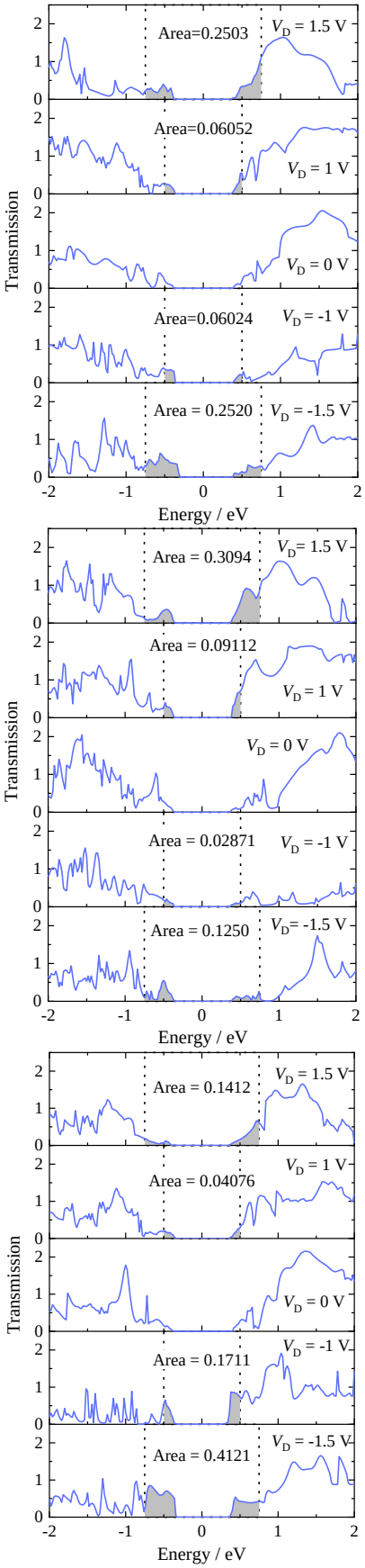

Fig. 4 The transmission spectrum of semiconducting Y-type zigzag branched carbon nanotube (8, 0)-(4, 0)-(4, 0) (source-drain-gate) under the bias voltage of 0 V, ±1 V, ±1.5 V. (a) V_G = 0 V, (b) V_G = -1 V, (c) V_G = 1 V

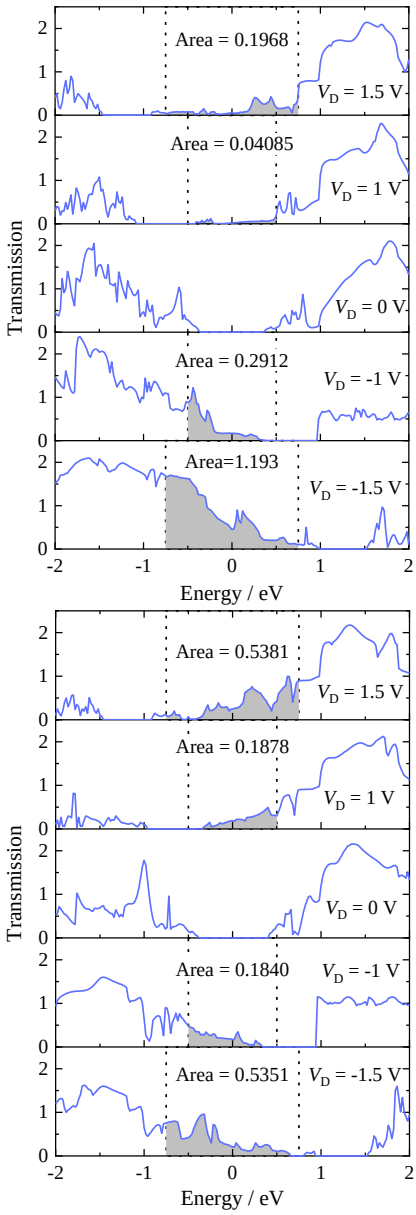

Fig. 5 The transmission spectrum of semiconducting Y-type zigzag branched carbon nanotube (8, 0)-(4, 0)-(4, 0) (drain- source-gate) under the bias voltage of 0 V, ±1 V, ±1.5 V. (a) V_G = 0 V, (b) V_G = -1 V, (c) V_G = 1 V

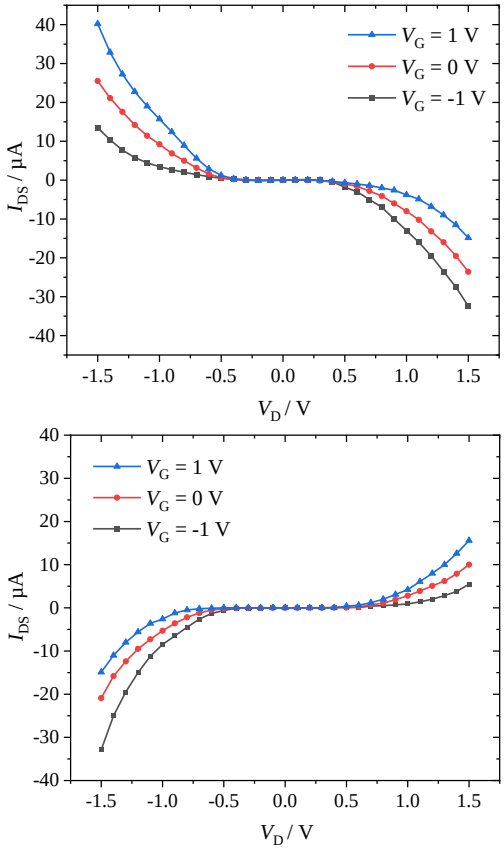

Fig. 6 The current-voltage(I-V) curve of semiconducting Y-type zigzag branched carbon nanotube (10, 0)-(5, 0)-(5, 0). (a) source, drain and gate: (10, 0), (5, 0) and (5, 0), and the inset shows the variation curve of k with V_D when V_G = 0 V, (b) source, drain and gate: (5, 0), (10, 0) and (5, 0), and the inset shows the variation curve of k with V_D when V_G = 0 V

As shown in Fig. 4(a), when V_G = 0 V and V_D = 0 V, there is a platform with transmission coefficient of 0 near the Fermi level, and the width is close to 0.5 eV. In particular, the change of bias window has no effect on the transmission coefficient platform. As the width of bias window increases, the transmission peaks on both sides of the Fermi level begin to enter the bias window, so that the integral area of the transmission spectrum is no longer zero. The number and height of transmission peaks entering the bias window increase with the increase of the bias window range. When V_D is 0 V, 1 V (-1 V) and 1.5 V (-1.5 V) respectively, the integral area of the transmission spectrum is 0, 0.06052 (0.06024) and 0.2503 (0.2520) respectively, the integral area and its increments also keep getting larger and are symmetrical about V_D = 0 V. This verify that the red circular curve in the range of V_D = [-0.5 V, 0.5 V] in Fig. 3(a), the value of | I_{DS} | is 0 μA and $|k|$ = 0, in the range of V_D = [-1.5V, -0.5 V] and [0.5 V, 1.5 V], as $|V_D|$ increases, $|I_{DS}|$ and $|k|$ increase continuously and both are symmetrical about V_D = 0 V. As shown in Figs. 4 (b) and 4(c), when V_G = ±1 V, the platform with a transmission coefficient of 0 hardly changes, and with the increase of the bias window width, the integral area and its increment also increasing, but no longer symmetric about V_D = 0 V. This verify that the blue triangle curve and black square curve in the range of V_D = [-0.5 V, 0.5 V] in Fig. 3(a), the value of $|I_{DS}|$ is 0 μA and $|k|$ = 0, in the range of V_D = [-1.5 V, -0.5 V] and [0.5 V, 1.5 V], as $|V_D|$ increases, $|I_{DS}|$ and $|k|$ increase continuously but are not symmetrical about V_D = 0 V.

As shown in Fig. 5(a), when V_G = 0 V and V_D = 0 V, a plateau with zero transmission coefficient exists near the Fermi level with the width close to 0.5 eV. In particular, as the width of the bias window increases, the transmission coefficient platform moves to the positive and negative directions, and the transmission peaks appear near the Fermi level, so that the integral area of the transmission spectrum is no longer zero. At the same time, the number and height of transmission peaks around the Fermi level increase with the increase of the bias window width. When

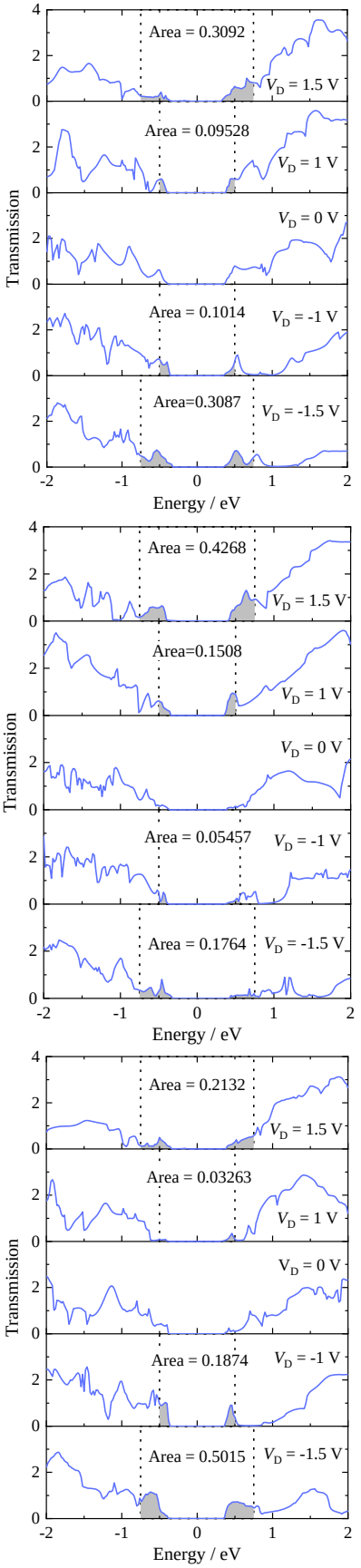

Fig. 7 The transmission spectrum of semiconducting Y-type zigzag branched carbon nanotube (10, 0)-(5, 0)-(5, 0) (source-drain-gate) under the bias voltage of 0 V, ±1 V, ±1.5 V. (a) V_G = 0 V, (b) V_G = -1 V, (c) V_G = 1 V

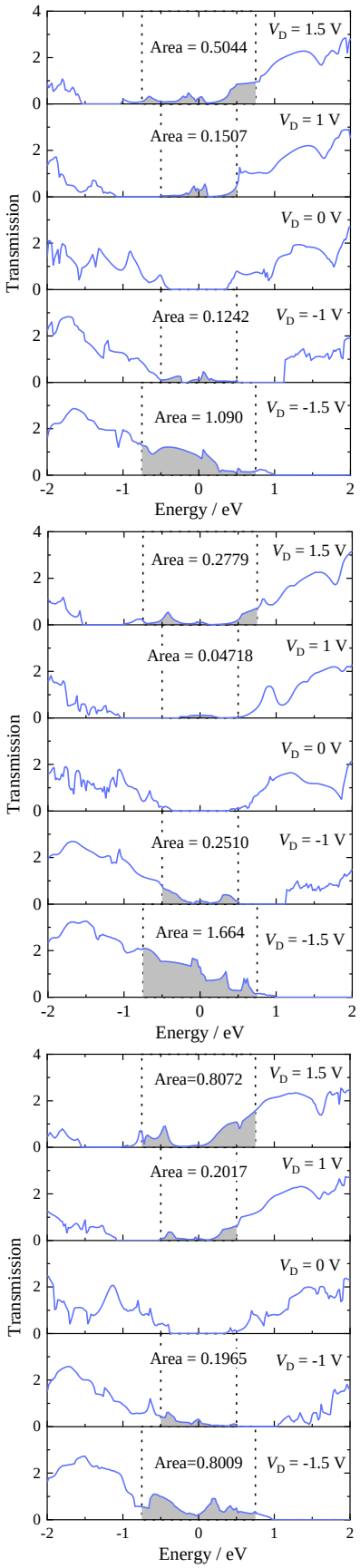

Fig. 8 The transmission spectrum of semiconducting Y-type zigzag branched carbon nanotube (10, 0)-(5, 0)-(5, 0) (drain- source-gate) under the bias voltage of 0 V, ±1 V, ±1.5 V. (a) V_G = 0 V, (b) V_G = -1 V, (c) V_G = 1 V

V_D is 0 V, 1 V (-1 V) and 1.5 V (-1.5 V) respectively, the integral areas are 0, 0.1223(0.2293), 0.4111(0.7600) respectively. The integral area and its increment are increasing but not symmetrical about V_D = 0 V. As shown in Figs. 5(b) and 5(c), when V_G = ± 1 V, with the increase of the bias window range, the platform with the transmission coefficient of zero near the Fermi level will also move to the positive and negative directions, and the number and height of transmission peaks in the bias window continue to increase, so the integral area and its increment also continue to increase. In particular, when V_G = 1 V and V_D is 0 V, 1 V (-1 V) and 1.5 V (-1.5 V), the integral area is symmetrical about V_D = 0 V, which are 0, 0.1878 (0.1840) and 0.5381 (0.5351) respectively. The above results verify the phenomenon in Fig. 3(b), when V_D = [-0.5 V, 0.5 V], $|I_{DS}|$ = 0 μA and k = 0, when V_D = [-1.5 V, -0.5 V] and [0.5 V, 1.5 V], $|I_{DS}|$ and k can be regulated by V_G, in particular, when V_G = 1 V, both $|I_{DS}|$ and k are symmetric about V_D = 0 V.

In order to research the effect of different diameters on the electronic transport properties of semiconducting Y-type zigzag branched carbon nanotubes, the carbon nanotube (10, 0)-(5, 0)-(5, 0) built from single-walled carbon nanotubes (10, 0) and (5, 0) with diameters of 7.83 and 3.91 respectively are selected as the research object. The current-voltage curves and transmission spectrum of the trunk (10, 0) used as the source and the two branches (5, 0) used as the drain and gate are showed in Figs. 6(a) and 7 respectively. The current-voltage curves and transmission spectrum of the trunk (10, 0) used as the drain and the two branches (5, 0) used as the source and gate are showed in Fig. 6(b) and Fig. 8 respectively. It can be seen from Figs. 6(a) and 6(b) that when V_G takes different values, the change trend of $|I_{DS}|$ is basically the same as that of $|I_{DS}|$ of semiconducting Y-type zigzag branched carbon nanotubes (8, 0)-(4, 0)-(4, 0), except that the current increases with the increase of diameter. The transmission spectrum in Figs. 7 and 8 verify the variation law of current-voltage curves in Fig. 6(a) and Fig. 6(b) respectively. Combined with Fig. 3, it can be shown that the diameter has no significant influence on the electronic transport properties between the branches of the semiconducting Y-type zigzag branched carbon nanotubes, and the current flowing through the other two branches can also be adjusted by the third end branch voltage.

For the purpose of investigating the influence of different conductivity on the electronic transport properties of Y-type zigzag branched carbon nanotubes, the metallic Y-type zigzag branched carbon nanotubes (12, 0)-(6, 0)-(6, 0) built from single-walled carbon nanotubes (12, 0) and (6, 0) with diameters of 9.39 and 4.70 respectively are selected as the research object, and the current-voltage curves are shown in Fig. 9. For the convenience of expressing the current-voltage linear relationship, $\bar{k}$ is defined as the slope of the current-voltage straight line, which is calculated by the following formula:

$$\bar{k} = \frac{\sum_{i=1}^{n} k}{n} \tag{4}$$

where n is the total number of current-voltage data.

The current-voltage curves of the trunk (12, 0) as the source and two branches (6, 0) as the drain and gate

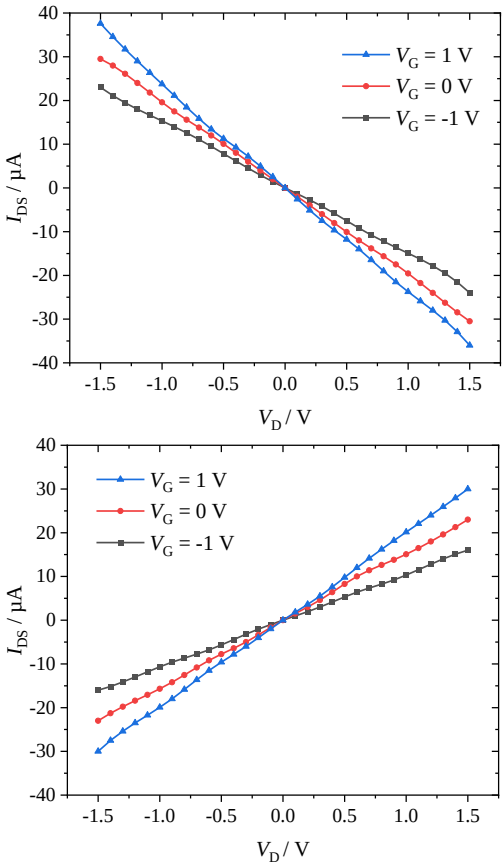

Fig. 9 The current-voltage(I-V) curve of metallic Y-type zigzag branched carbon nanotube (12, 0)-(6, 0)-(6, 0). (a) source, drain and gate: (12, 0), (6, 0) and (6, 0), (b) source, drain and gate: (6, 0), (12, 0) and (6, 0)

respectively are showed in Fig. 9(a), which shows a linear downward trend as a whole, and I_{DS} is symmetrical about (0, 0). When V_G is taken as -1 V, 0 V and 1 V in turn, the absolute value of the slope of the current-voltage straight line $|\bar{k}|$ increases continuously, which are 15.8, 19.9 and 24.7 respectively. The current-voltage curves of the trunk (12, 0) as the drain and two branches (6, 0) as the source and gate respectively are showed in Fig. 9(b). The overall trend is linear, and I_{DS} is also symmetrical about (0, 0). When V_G is taken as -1 V, 0 V and 1 V in turn, $|\bar{k}|$ will also increase, which are 10.6, 15.3 and 20.1 respectively. The research results show that the current between the branches of the metallic Y-type zigzag branched carbon nanotubes changes linearly, and the gate voltage can also be used to control the current flowing through the drain-source.

In order to further analyze the variation law of the current-voltage curves in Figs. 9(a) and 9(b), the transmission spectrum of the trunk (12, 0) as the source and the two branches (6, 0) as the drain and gate respectively when V_G takes 0 V, -1 V and 1 V is showed in Figs. 10(a)-(c). The transmission spectrum of the trunk (12, 0) as the drain and the two branches (6, 0) as the source and gate respectively when V_G takes 0 V, -1 V and 1 V is showed in Figs. 11(a)-(c). The black dotted line represents the boundary of the bias window, and the gray shaded area represents the integral area of the transmission coefficient in the bias window.

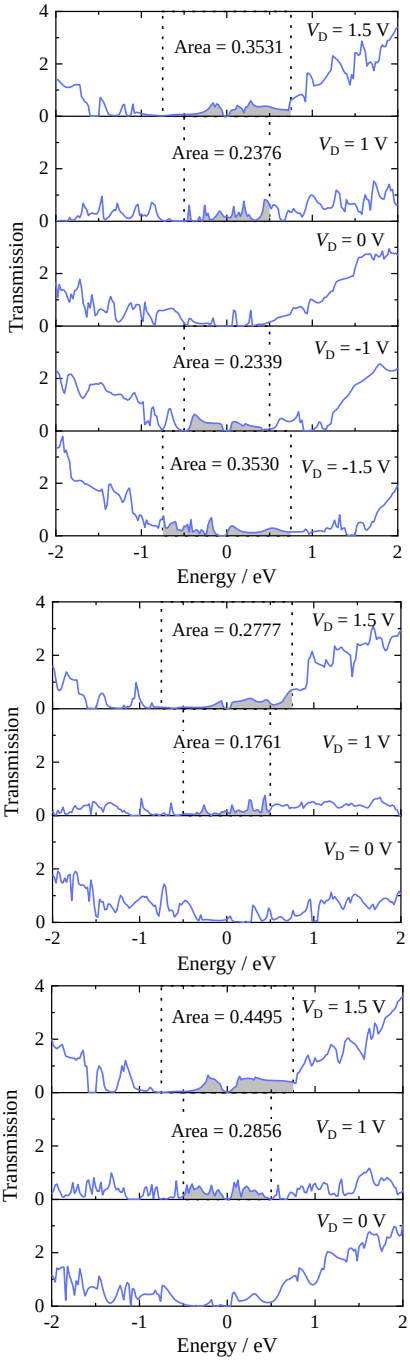

Fig. 10 The transmission spectrum of metallic Y-type zigzag branched carbon nanotube (12, 0)-(6, 0)-(6, 0) (source-drain-gate) under the bias voltage of 0 V, ±1 V, ±1.5 V: (a) VG = 0 V, under the bias voltage of 0 V, 1 V, 1.5 V: (b) VG = -1 V, (c) VG = 1 V

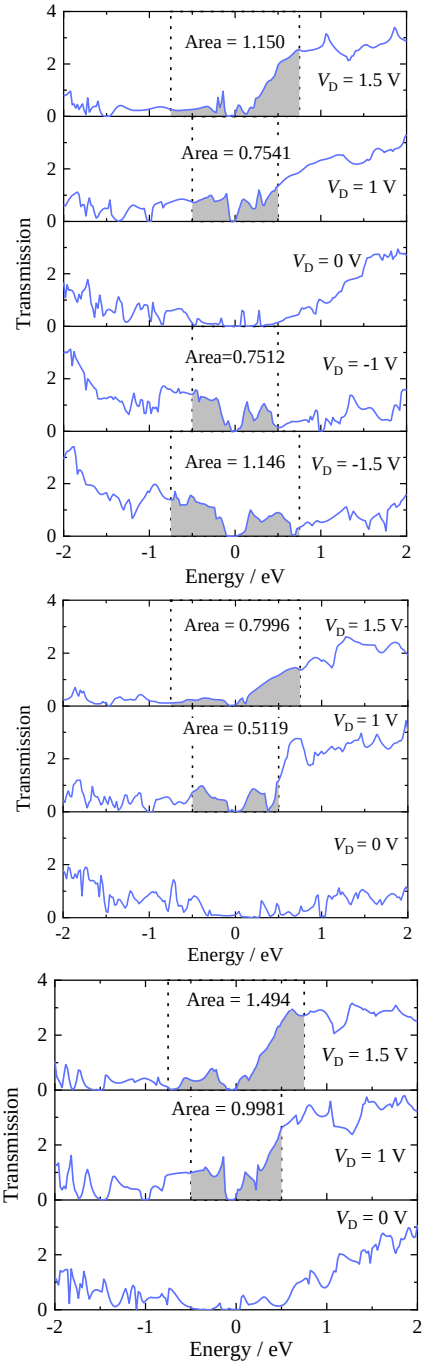

Fig. 11 The transmission spectrum of metallic Y-type zigzag branched carbon nanotube (12, 0)-(6, 0)-(6, 0) (drain-source-gate) under the bias voltage of 0 V, ±1 V, ±1.5 V: (a) V_G = 0 V, under the bias voltage of 0 V, 1 V, 1.5 V: (b) V_G = -1 V, (c) V_G = 1 V.

As shown in Fig. 10(a), there is no platform with transmission coefficient of 0 near the Fermi level, so when the range of the bias window is expanded, the integral area will continue to increase with the increase of the number and height of transmission peaks. When V_D is taken as 0 V, 1 V (-1 V) and 1.5 V (-1.5 V), the integral areas are 0, 0.2376 (0.2339) and 0.3531 (0.3530) respectively, which are symmetrical about V_D = 0 V and the integral area increment does not change. The change law is same in Fig. 10(a)-(c), but in the same range of bias window, the integral area increases with the increase of V_G. The above research results verify that the I_{DS} in Fig. 9(a) changes linearly and is symmetrical about (0, 0), and $|\bar{k}|$ can be changed through V_G, so as to realize the regulation of I_{DS}. By analyzing and comparing the data in Fig. 11, the variation law of I_{DS} in Fig. 9(b) can also be verified, that is, the I_{DS} in Fig. 9(b) changes linearly and is symmetrical about (0, 0), and $|\bar{k}|$ can be changed by V_G, thereby regulating the I_{DS}.

4. Conclusions

In this study, single-walled carbon nanotubes with various conductivities and diameters are connected to create Y-type zigzag branching carbon nanotubes. The electrical transport characteristics between the branches of Y-type zigzag branched carbon nanotubes are investigated using a semi-empirical calculation approach integrating tight-binding density functional theory and non-equilibrium Green's function. The findings demonstrate that the semiconducting Y-type zigzag branched carbon nanotubes with various diameters (8, 0)-(4, 0)-(4, 0) and (10, 0)-(5, 0)-(5, 0) have the same electron transport properties between the branches. Additionally, the drain-source current is in the cut-off state in the bias voltage range [-0.5 V, 0.5 V] and is unaffected by the gate voltage. The drain-source current, however, exhibits a nonlinear decreasing trend between [-1.5 V, -0.5 V] and [0.5 V, 1.5 V]. By adjusting the gate voltage, the current may be controlled, under negative bias voltage, the regulatory impact is stronger. The current exhibits a nonlinear increasing trend and other modifications are constant whether the branch locations where the drain and source are placed are switched. In the whole [-1.5 V, 1.5 V] range, the drain-source current of metallic Y-type zigzag-branched carbon nanotubes (12,0) - (6,0) - (6,0) exhibits a linear downward trend and is symmetrical around (0, 0). The current may be controlled by adjusting the gate voltage. Change the branch where the source drain is situated, and the other alterations are the same while the current displays a linear rising trend. A theoretical foundation for the use of branching carbon nanotubes in molecular devices, logic circuits, or carbon-based nano electronic devices is provided by the findings discussed above in the study.

Acknowledgment

Project supported by the National Key Research and Development Program of China (2018YFB1309200), the National Natural Science Foundation of China (Grant Nos 61573238).

References

Adamian, A., Safari, K.H., Sheikholeslami, M., Habibi, M., Al-Furjan, M. and Chen, G. (2020), "Critical temperature and frequency characteristics of GPLs-reinforced composite doubly curved panel", *Appl. Sci.*, **10**(9), 3251. https://doi.org/10.3390/app10093251.

Akbas, S.D. (2018), "Forced vibration analysis of cracked functionally graded microbeams", *Adv. Nano Res.*, **6**(1), 39. http://doi.org/10.12989/anr.2018.6.1.039.

Akbaş, Ş.D. (2018), "Bending of a cracked functionally graded nanobeam", *Adv. Nano Res.*, **6**(3), 219. http://doi.org/10.12989/anr.2018.6.3.219.

Al-Furjan, M., Dehini, R., Khorami, M., Habibi, M. and won Jung, D. (2020a), "On the dynamics of the ultra-fast rotating cantilever orthotropic piezoelectric nanodisk based on nonlocal strain gradient theory", *Compos. Struct.*, 112990. https://doi.org/10.1016/j.compstruct.2020.112990.

Al-Furjan, M., Fereidouni, M., Habibi, M., Abd Ali, R., Ni, J. and Safarpour, M. (2020b), "Influence of in-plane loading on the vibrations of the fully symmetric mechanical systems via dynamic simulation and generalized differential quadrature framework", *Eng. Comput.*, 1-23. https://doi.org/10.1007/s00366-020-01177-7.

Allahkarami, F., Nikkhah-Bahrami, M. and Saryazdi, M.G. (2017), "Damping and vibration analysis of viscoelastic curved microbeam reinforced with FG-CNTs resting on viscoelastic medium using strain gradient theory and DQM", *Steel Compos. Struct.*, **25**(2), 141-155. https://doi.org/10.12989/scs.2017.25.2.141.

Andriotis, A.N., Menon, M., Srivastava, D. and Chernozatonskii, L. (2001), "Rectification properties of carbon nanotube "Y-junctions", *Phys. Rev. Lett.*, **87**(6), 066802. https://doi.org/10.1103/PhysRevLett.87.066802.

Araujo, F.R.V., da Costa, D.R., Lima, F.N., Nascimento, A.C.S. and Pereira, J.M., Jr. (2021), "Gate potential-controlled current switching in graphene Y-junctions", *J. Phys. Condens. Matter.*, **33**(37), 375501. https://doi.org/10.1088/1361-648X/ac0f2b.

Arefi, M. and Zenkour, A.M. (2018), "Free vibration analysis of a three-layered microbeam based on strain gradient theory and three-unknown shear and normal deformation theory", *Steel Compos. Struct.*, **26**(4), 421-437. https://doi.org/10.12989/scs.2018.26.4.421.

Aydogdu, M., Arda, M. and Filiz, S. (2018), "Vibration of axially functionally graded nano rods and beams with a variable nonlocal parameter", *Adv. Nano Res.*, **6**(3), 257. http://doi.org/10.12989/anr.2018.6.3.257.

Azimi, M., Mirjavadi, S.S., Shafiei, N. and Hamouda, A.M.S. (2016), "Thermo-mechanical vibration of rotating axially functionally graded nonlocal Timoshenko beam", *Appl. Phys. A.*, **123**(1), 104. https://doi.org/10.1007/s00339-016-0712-5.

Bai, Y.X., Zhang, R.F., Ye, X., Zhu, Z.X., Xie, H.H., Shen, B.Y., Cai, D., Liu, B.F., Zhang, C.X., Jia, Z., Zhang, S.l., Li, X.D. and Wei, F. (2018), "Carbon nanotube bundles with tensile strength over 80 GPa", *Nature Nanotechnol.*, **13**(7), 589-595. https://doi.org/10.1038/s41565-018-0141-z.

Bandaru, P.R., Daraio, C., Jin, S. and Rao, A.M. (2005), "Novel electrical switching behaviour and logic in carbon nanotube Y-junctions", *Nature Mater.*, **4**(9), 663-666. https://doi.org/10.1038/nmat1450.

Bensaid, I., Bekhadda, A. and Kerboua, B. (2018), "Dynamic analysis of higher order shear-deformable nanobeams resting on elastic foundation based on nonlocal strain gradient theory", *Adv. Nano Res.*, **6**(3), 279. http://doi.org/10.12989/anr.2018.6.3.279.

Butti, P., Shorubalko, I., Sennhauser, U. and Ensslin, K. (2013), "Finite element simulations of graphene based three-terminal nanojunction rectifiers", *J. Appl. Phys.*, **114**(3), 033710. https://doi.org/10.1063/1.4815956.

Buttiker, M., Imry, Y., Landauer, R. and Pinhas, S. (1985), "Generalized many-channel conductance formula with application to small rings", *Phys. Rev. B*, **31**(10), 6207-6215. https://doi.org/10.1103/physrevb.31.6207.

ChandraKishore, S. and Pandurangan, A. (2013), "Synthesis and characterization of Y-shaped carbon nanotubes using Fe/AlPO4 catalyst by CVD", *Chem. Eng. J.*, **222**, 472-477. https://doi.org/10.1016/j.cej.2013.02.070.

Charlier, J.C., Ebbesen, T.W. and Lambin, P. (1996), "Structural and electronic properties of pentagon-heptagon pair defects in carbon nanotubes", *Phys. Rev. B*, **53**(16), 11108-11113. https://doi.org/10.1103/physrevb.53.11108.

Chen, L., Zhao, Y., Jing, J. and Hou, H. (2023), "Microstructural evolution in graphene nanoplatelets reinforced magnesium matrix composites fabricated through thixomolding process", *J. Alloys Compd.*, **940**, 168824.

https://doi.org/10.1016/j.jallcom.2023.168824.
Chen, Q.L., Wu, X.J., Cheng, H.Y., Li, Q. and Chen, S. (2019), "Facile synthesis of carbon nanobranches towards cobalt ion sensing and high-performance micro-supercapacitors", *Nanosc. Adv.*, **1**(9), 3614-3620. https://doi.org/10.1039/c9na00181f.
Cheng, F., Niu, B., Xu, N., Zhao, X. and Ahmad, A.M. (2023), "Fault detection and performance recovery design with deferred actuator replacement via a low-computation method", *IEEE T Automat. Sci. Eng.*, 1-11. https://doi.org/10.1109/TASE.2023.3300723.
Chico, L., Crespi, V.H., Benedict, L.X., Louie, S.G. and Cohen, M.L. (1996), "Pure carbon nanoscale devices nanotube heterojunctions", *Phys. Rev. Lett.*, **76**(6), 971. https://doi.org/10.1103/PhysRevLett.76.971.
Dai, Z., Zhang, L., Bolandi, S.Y. and Habibi, M. (2021), "On the vibrations of the non-polynomial viscoelastic composite open-type shell under residual stresses", *Compos. Struct.*, 113599. https://doi.org/10.1016/j.compstruct.2021.113599.
Ding, H.Y., Shi, C.Y., Ma, L., Yang, Z., Wang, M.Y., Wang, Y.Q., Chen, T., Sun, L.N. and Toshio, F. (2018), "Visual servoing-based nanorobotic system for automated electrical characterization of nanotubes inside SEM", *Sensors*. **18**(4), 1137. https://doi.org/10.3390/s18041137.
Durkop, T., Getty, S.A., Cobas, E. and Fuhrer, M.S. (2004), "Extraordinary mobility in semiconducting carbon nanotubes", *Nano Lett.*, **4**(1), 35-39. https://doi.org/10.1021/nl034841q.
Ebrahimi, F., Kokaba, M., Shaghaghi, G. and Selvamani, R. (2020), "Dynamic characteristics of hygro-magneto-thermo-electrical nanobeam with non-ideal boundary conditions", *Adv. Nano Res.*, **8**(2), 169-182. https://doi.org/10.12989/anr.2020.8.2.169.
Ebrahimi, F., Shafiei, N., Kazemi, M. and Mousavi Abdollahi, S.M. (2017), "Thermo-mechanical vibration analysis of rotating nonlocal nanoplates applying generalized differential quadrature method", *Mech. Adv. Mater. Struct.*, **24**(15), 1257-1273. https://doi.org/10.1080/15376494.2016.1227499.
Ehyaei, J., Akbarshahi, A. and Shafiei, N. (2017), "Influence of porosity and axial preload on vibration behavior of rotating FG nanobeam", *Adv. Nano Res.*, **5**(2), 141. https://doi.org/10.12989/anr.2017.5.2.141.
Gafour, Y., Hamidi, A., Benahmed, A., Zidour, M. and Bensattalah, T. (2020), "Porosity-dependent free vibration analysis of FG nanobeam using non-local shear deformation and energy principle", *Adv. Nano Res.*, **8**(1), 37-47. https://doi.org/10.12989/anr.2020.8.1.037.
Ghadiri, M., Hosseini, S.H.S. and Shafiei, N. (2016a), "A power series for vibration of a rotating nanobeam with considering thermal effect", *Mech. Adv. Mater. Struct.*, **23**(12), 1414-1420. https://doi.org/10.1080/15376494.2015.1091527.
Ghadiri, M., Shafiei, N. and Alavi, H. (2017a), "Thermo-mechanical vibration of orthotropic cantilever and propped cantilever nanoplate using generalized differential quadrature method", *Mech. Adv. Mater. Struct.*, **24**(8), 636-646. https://doi.org/10.1080/15376494.2016.1196770.
Ghadiri, M., Shafiei, N. and Alireza Mousavi, S. (2016b), "Vibration analysis of a rotating functionally graded tapered microbeam based on the modified couple stress theory by DQEM", *Appl. Phys. A*, **122**(9), 837. https://doi.org/10.1007/s00339-016-0364-5.
Ghadiri, M., Shafiei, N. and Babaei, R. (2017b), "Vibration of a rotary FG plate with consideration of thermal and Coriolis effects", *Steel Compos. Struct.*, **25**(2), 197-207. https://doi.org/10.12989/scs.2017.25.2.197.
Ghadiri, M., Shafiei, N. and Hossein Alavi, S. (2017c), "Vibration analysis of a rotating nanoplate using nonlocal elasticity theory", *J. Solid Mech.*, **9**(2), 319-337.
Gu Yun-Feng, Wu Xiao-Li and Hong-Zhang, W. (2016), "Ballistic thermal rectification in the three-terminal graphene nano-junction with asymmetric connection angle", *Acta Phys. Sin.*, **65**(24), 248104. https://doi.org/10.7498/aps.65.248104.
Guo, S., Zhao, X., Wang, H. and Xu, N. (2023), "Distributed consensus of heterogeneous switched nonlinear multiagent systems with input quantization and DoS attacks", *Appl. Math. Comput.*, **456**, 128127. https://doi.org/10.1016/j.amc.2023.128127.
Hamidi, A., Houari, M.S.A., Mahmoud, S. and Tounsi, A. (2015), "A sinusoidal plate theory with 5-unknowns and stretching effect for thermomechanical bending of functionally graded sandwich plates", *Steel Compos. Struct.*, **18**(1), 235-253. https://doi.org/10.12989/scs.2015.18.1.235.
Händel, B., Hähnlein, B., Göckeritz, R., Schwierz, F. and Pezoldt, J. (2014), "Electrical gating and rectification in graphene three-terminal junctions", *Appl. Surf. Sci.*, **291**, 87-92. https://doi.org/10.1016/j.apsusc.2013.09.066.
Hills, G., Lau, C., Wright, A., Fuller, S., Bishop, M.D., Srimani, T., Kanhaiya, P., Ho, R., Amer, A., Stein, Y., Murphy, D., Arvind, Chandrakasan, A. and Shulaker, M.M. (2019), "Modern microprocessor built from complementary carbon nanotube transistors", *Nature*, **572**(7771), 595-602. https://doi.org/10.1038/s41586-019-1493-8.
Hou, F., Wu, S., Moradi, Z. and Shafiei, N. (2021), "The computational modeling for the static analysis of axially functionally graded micro-cylindrical imperfect beam applying the computer simulation", *Eng. Comput.*, 1-19. https://doi.org/10.1007/s00366-021-01456-x.
Huang, K., Xu, Q., Ying, Q., Gu, B. and Yuan, W. (2023a), "Wireless strain sensing using carbon nanotube composite film", *Compos. Part B Eng.*, **256**, 110650. https://doi.org/10.1016/j.compositesb.2023.110650.
Huang, S., Zong, G., Wang, H., Zhao, X. and Alharbi, K.H. (2023b), "Command filter-based adaptive fuzzy self-triggered control for MIMO nonlinear systems with time-varying full-state constraints", *Int. J. Fuzzy Syst.*, 1-18. https://doi.org/10.1007/s40815-023-01560-8.
Huang, X., Zhang, Y., Moradi, Z. and Shafiei, N. (2021), "Computer simulation via a couple of homotopy perturbation methods and the generalized differential quadrature method for nonlinear vibration of functionally graded non-uniform micro-tube", *Eng. Comput.*, 1-18. https://doi.org/10.1007/s00366-021-01395-7.
Javey, A., Guo, J., Wang, Q., Lundstrom, M. and Dai, H.J. (2003), "Ballistic carbon nanotube field-effect transistors", *Nature*, **424**(6949), 654-657. https://doi.org/10.1038/nature01797.
Joseph Berkmans, A., Jagannatham, M., Priyanka, S. and Haridoss, P. (2014), "Synthesis of branched, nano channeled, ultrafine and nano carbon tubes from PET wastes using the arc discharge method", *Waste Manag.*, **34**(11), 2139-2145. https://doi.org/10.1016/j.wasman.2014.07.004.
Kim, W.Y. and Kim, K.S. (2008), "Carbon nanotube, graphene, nanowire, and molecule-based electron and spin transport phenomena using the nonequilibrium Green's function method at the level of first principles theory", *J. Comput. Chem.*, **29**(7), 1073-1083. https://doi.org/10.1002/jcc.20865.
Li, M., Guo, Q., Chen, L., Li, L., Hou, H. and Zhao, Y. (2022), "Microstructure and properties of graphene nanoplatelets reinforced AZ91D matrix composites prepared by electromagnetic stirring casting", *J. Mater. Res. Technol.*, **21**, 4138-4150. https://doi.org/10.1016/j.jmrt.2022.11.033.
Li, Y., Li, S., Guo, K., Fang, X. and Habibi, M. (2020), "On the modeling of bending responses of graphene-reinforced higher order annular plate via two-dimensional continuum mechanics approach", *Eng. Comput.*, 1-22. https://doi.org/10.1007/s00366-020-01166-w.
Lin, Y.N., Ma, L., Yang, Q., Geng, S.C., Ye, M.-S., Chen, T. and

Sun, L.N. (2022), "Electron transport properties of carbon nanotubes with radial compression deformation", *Acta Phys. Sin.*, **71**(2), 027301. https://doi.org/10.7498/aps.71.20211370.

Liu, B., Zhou, H., Jin, H., Zhu, J., Wang, Z., Hu, C., Liang, L., Mu, S. and He, D. (2021), "A new strategy to access Co/N co-doped carbon nanotubes as oxygen reduction reaction catalysts", *Chinese Chem. Lett.*, **32**(1), 535-538. https://doi.org/10.1016/j.cclet.2020.04.002.

Martel, R., Schmidt, T., Shea, H.R., Hertel, T. and Avouris, P. (1998), "Single- and multi-wall carbon nanotube field-effect transistors", *Appl. Phys. Lett.*, **73**(17), 2447-2449. https://doi.org/10.1063/1.122477.

Matouk, H., Bousahla, A.A., Heireche, H., Bourada, F., Bedia, E., Tounsi, A., Mahmoud, S., Tounsi, A. and Benrahou, K. (2020), "Investigation on hygro-thermal vibration of P-FG and symmetric S-FG nanobeam using integral Timoshenko beam theory", *Adv. Nano Res.*, **8**(4), 293-305. https://doi.org/10.12989/anr.2020.8.4.293.

Navi, B.R., Mohammadimehr, M. and Arani, A.G. (2019), "Active control of three-phase CNT/resin/fiber piezoelectric polymeric nanocomposite porous sandwich microbeam based on sinusoidal shear deformation theory", *Steel Compos. Struct.*, **32**(6), 753-767. https://doi.org/10.12989/scs.2019.32.6.753.

Ohnishi, M., Suzuki, K. and Miura, H. (2016), "Effects of uniaxial compressive strain on the electronic-transport properties of zigzag carbon nanotubes", *Nano Res.*, **9**(5), 1267-1275. https://doi.org/10.1007/s12274-016-1022-0.

Ouyang, M., Huang, J.L., Cheung, C.L. and Lieber, C.M. (2001), "Atomically resolved single-walled carbon nanotube intramolecular junctions", *Science*, **291**(5501), 97-100. https://doi.org/10.1126/science.291.5501.97.

Park, J., Daraio, C., Jin, S., Bandaru, P.R., Gaillard, J. and Rao, A.M. (2006), "Three-way electrical gating characteristics of metallic Y-junction carbon nanotubes", *Appl. Phys. Lett.*, **88**(24), 243113. https://doi.org/10.1063/1.2213013.

Pecchia, A., Penazzi, G., Salvucci, L. and Di Carlo, A. (2008), "Non-equilibrium Green's functions in density functional tight binding: method and applications", *New J. Phys.*, **10**(6), 065022. https://doi.org/10.1088/1367-2630/10/6/065022.

Peng, L.M., Zhang, Z.Y. and Qiu, C.G. (2019), "Carbon nanotube digital electronics", *Nature Electron.*, **2**(11), 499-505. https://doi.org/10.1038/s41928-019-0330-2.

Pitner, G., Hills, G., Llinas, J.P., Persson, K.M., Park, R., Bokor, J., Mitra, S. and Wong, H.P. (2019), "Low-temperature side contact to carbon nanotube transistors: Resistance distributions down to 10 nm contact length", *Nano Lett.*, **19**(2), 1083-1089. https://doi.org/10.1021/acs.nanolett.8b04370.

Seifert, G. (2007), "Tight-binding density functional theory: An approximate Kohn−Sham DFT scheme", *J. Phys. Chem. A*, **111**(26), 5609-5613. https://doi.org/10.1021/jp069056r.

Shafiei, N., Ghadiri, M., Makvandi, H. and Hosseini, S.A. (2017), "Vibration analysis of Nano-Rotor's Blade applying Eringen nonlocal elasticity and generalized differential quadrature method", *Appl. Math. Modell.*, **43**, 191-206. https://doi.org/10.1016/j.apm.2016.10.061.

Shafiei, N., Hamisi, M. and Ghadiri, M. (2020), "Vibration analysis of rotary tapered axially functionally graded timoshenko nanobeam in thermal environment", *J. Solid Mech.*, **12**(1), 16-32. https://doi.org/10.22034/jsm.2019.563759.1273.

Shafiei, N., Kazemi, M. and Ghadiri, M. (2016), "Nonlinear vibration behavior of a rotating nanobeam under thermal stress using Eringen's nonlocal elasticity and DQM", *Appl. Phys. A*, **122**(8), 728. https://doi.org/10.1007/s00339-016-0245-y.

Shahabinejad, E., Shafiei, N. and Ghadiri, M. (2018), "Influence of temperature change on modal analysis of rotary functionally graded nano-beam in thermal environment", *J. Solid Mech.*, **10**(4), 779-803. https://jsm.arak.iau.ir/article_545719.html.

Shen, S., Han, C., Wang, B. and Wang, Y. (2022), "Engineering d-band center of nickel in nickel@nitrogen-doped carbon nanotubes array for electrochemical reduction of CO2 to CO and Zn-CO2 batteries", *Chinese Chem. Lett.*, **33**(8), 3721-3725. https://doi.org/10.1016/j.cclet.2021.10.063.

Shivanian, E., Ghadiri, M. and Shafiei, N. (2017), "Influence of size effect on flapwise vibration behavior of rotary microbeam and its analysis through spectral meshless radial point interpolation", *Appl. Phys. A*, **123**(5), 329. https://doi.org/10.1007/s00339-017-0955-9.

Sun, Y., Peng, Z.S., Li, H.M., Wang, Z.Q., Mu, Y.Q., Zhang, G.P., Chen, S., Liu, S.Y., Wang, G.T., Liu, C.D., Sun, L.F., Man, B.Y. and Yang, C. (2019), "Suspended CNT-Based FET sensor for ultrasensitive and label-free detection of DNA hybridization", *Biosens. Bioelectr.*, **137**, 255-262. https://doi.org/10.1016/j.bios.2019.04.054.

Tang, F., Wang, H., Zhang, L., Xu, N. and Ahmad, A.M. (2023), "Adaptive optimized consensus control for a class of nonlinear multi-agent systems with asymmetric input saturation constraints and hybrid faults", *Commun. Nonlinear Sci. Numer. Simul.*, **126**, 107446. https://doi.org/10.1016/j.cnsns.2023.107446.

Wang, H., Chang, S., Hu, Y., He, H.Y., He, J., Huang, Q.J., He, F. and Wang, G.F. (2014), "A novel barrier controlled tunnel FET", *IEEE Electr. Device Lett.*, **35**(7), 798-800. https://doi.org/10.1109/led.2014.2325058.

Wang, P., Gao, Z., Pan, F., Moradi, Z., Mahmoudi, T. and Khadimallah, M.A. (2022), "A couple of GDQM and iteration techniques for the linear and nonlinear buckling of bi-directional functionally graded nanotubes based on the nonlocal strain gradient theory and high-order beam theory", *Eng. Anal. Bound. Elem.*, **143**, 124-136. https://doi.org/10.1016/j.enganabound.2022.06.007.

Wang Yi-Jun and Cheng, Y. (2015), "Field-emission current densities of carbon nanotube under the different electric fields", *Acta Phys. Sin.*, **64**(19), 197304. https://doi.org/10.7498/aps.64.197304.

Wang, Y.Z., Ma, L., Yang, Q., Geng, S.C., Lin, Y.N., Chen, T. and Sun, L.N. (2020), "Length-controllable picking method and conductivity analysis of carbon nanotubes", *Acta Phys. Sin.*, **69**(6), 068801. https://doi.org/10.7498/aps.69.20191298.

Wang, Z., Dai, L., Yao, J., Guo, T., Hrynsphan, D., Tatsiana, S. and Chen, J. (2021), "Enhanced adsorption and reduction performance of nitrate by Fe–Pd–Fe3O4 embedded multi-walled carbon nanotubes", *Chemosphere*, **281**, 130718. https://doi.org/10.1016/j.chemosphere.2021.130718.

Wu, W., Xu, N., Niu, B., Zhao, X. and Ahmad, A.M. (2023), "Low-computation adaptive saturated self-triggered tracking control of uncertain networked systems", *Electronics*, **12**(13), 2771. https://doi.org/10.3390/electronics12132771

Xin, Z., Zhao, X., Ji, H., Ma, T., Li, H., Zhong, S. and Shen, Z. (2021), "Amorphous carbon-linked TiO2/carbon nanotube film composite with enhanced photocatalytic performance: The effect of interface contact and hydrophilicity", *Chinese Chem. Lett.*, **32**(7), 2151-2154. https://doi.org/10.1016/j.cclet.2020.11.054.

Xu, L., Qiu, C.G., Peng, L.M. and Zhang, Z.Y. (2020), "Suppression of leakage current in carbon nanotube field-effect transistors", *Nano Res.*, **14**(4), 976-981. https://doi.org/10.1007/s12274-020-3135-8.

Xu, W., Pan, G., Moradi, Z. and Shafiei, N. (2021), "Nonlinear forced vibration analysis of functionally graded non-uniform cylindrical microbeams applying the semi-analytical solution", *Compos. Struct.*, 114395. https://doi.org/10.1016/j.compstruct.2021.114395.

Xue, B.C., Shao, X.G. and Cai, W.S. (2008), "Structures and stabilities of multi-terminal carbon nanotube junctions",

Comput. Mater. Sci., **43**(3), 531-539. https://doi.org/10.1016/j.commatsci.2007.12.020.

Yang, H., Huang, H., Liu, X., Li, Z., Li, J., Zhang, D., Chen, Y. and Liu, J. (2023), "Sensing mechanism of an Au-TiO2-Ag nanograting based on Fano resonance effects", *Appl. Opt.*, **62**(17), 4431-4438. https://doi.org/10.1364/AO.491732.

Yang, Q., Ma, L., Geng, S.C., Lin, Y.N., Chen, T. and Sun, L.N. (2021a), "Molecular dynamics simulation of contact behaviors between multiwall carbon nanotube and metal surface", *Acta Phys. Sin.*, **70**(10), 222-234. https://doi.org/10.7498/aps.70.20202194.

Yang, Q., Ma, L., Xiao, S., Zhang, D., Djoulde, A., Ye, M., Lin, Y., Geng, S., Li, X., Chen, T. and Sun, L. (2021b), "Electrical conductivity of multiwall carbon nanotube bundles contacting with metal electrodes by nano manipulators inside SEM", *Nanomaterials*, **11**(5). https://doi.org/10.3390/nano11051290.

Zare, R., Najaafi, N., Habibi, M., Ebrahimi, F. and Safarpour, H. (2020), "Influence of imperfection on the smart control frequency characteristics of a cylindrical sensor-actuator GPLRC cylindrical shell using a proportional-derivative smart controller", *Smart Struct. Syst.*, **26**(4), 469-480. https://doi.org/10.12989/sss.2020.26.4.469.

Zhao, C., Yin, X., Guo, Z., Zhao, D., Yang, G., Chen, A., Fan, L., Zhang, Y. and Zhang, N. (2021), "High lithiophilic nitrogen-doped carbon nanotube arrays prepared by in-situ catalyze for lithium metal anode", *Chinese Chem. Lett.*, **32**(7), 2254-2258. https://doi.org/10.1016/j.cclet.2020.12.056.

Zhao, W., Suo, H., Wang, S., Ma, L., Wang, L., Wang, Q. and Zhang, Z. (2022), "Mg gas infiltration for the fabrication of MgB2 pellets using nanosized and microsized B powders", *J. Eur. Ceram. Soc.*, **42**(15), 7036-7048. https://doi.org/10.1016/j.jeurceramsoc.2022.08.029.

Zhao, Y., Niu, B., Zong, G., Zhao, X. and Alharbi, K.H. (2023), "Neural network-based adaptive optimal containment control for non-affine nonlinear multi-agent systems within an identifier-actor-critic framework", *J. Franklin Inst.*, **360**(12), 8118-8143. https://doi.org/10.1016/j.jfranklin.2023.06.014.

JL